Appl. Phys. A 64, 155–159 (1997)

Applied Physics A Materials Science & Processing

Evaluation of thermal conductivity of porous silicon layers by a photoacoustic method

G. Benedetto, L. Boarino, R. Spagnolo

Istituto Elettrotecnico Nazionale Galileo Ferraris, Strada delle Cacce 91, 10135 Torino, Italy
(Fax: + 39-11/346384, E-mail: gbenedet@ac.ien.it)

Received: 4 July 1996/Accepted: 13 August 1996

Abstract. The paper shows that it is possible to evaluate the thermal conductivity of porous silicon layers by a conventional photoacoustic gas-microphone technique, on the basis of a simple interpretative model for stratified samples.

Samples produced by electrochemical etching of crystalline wafers of different type and thickness are considered. The frequency variation of photoacoustic signal, in amplitude and phase, is studied and interpreted by means of a four-layers (air, porous silicon, crystalline silicon, air) model. Thermal conductivity values in the range 2.5–31.2 W/m K are obtained.

PACS: 43.35; 65

Porous Silicon (PS) is a very promising material in Si technology. It was discovered in 1956 [1] and since then intensively studied particularly after finding its strong photoluminescence [2], which has suggested many potential optoelectronic applications. One of the main application in other technological sectors [3, 4] is its use for structures with specific thermal properties in sensors where it is necessary to get high thermal insulation in order to obtain a large temperature variation in correspondence of a small amount of heat. Examples are thermal infrared sensors (bolometers and thermocouples) and thermal gas sensors.

In last years, micromachining has been widely used to obtain thermally insulated structures, as free-standing membranes or bridges [5, 6]. Usually single-crystal silicon itself cannot be used in reason of its high thermal conductivity (approximately 150 W/m K). However silicon oxide, nitride, carbide membranes can be employed owing to their much lower thermal conductivity.

The micromechanical technology more often used is backside etching of the wafer in KOH solution; alternatively, the free membrane can be obtained by using a thick sacrificial layer. These structures have the advantage of a low thermal conductance but the evident disadvantage of mechanical vulnerability.

A different approach can consist in depositing the sensor sensitive area on a PS layer 50 μm or more thick, which acts itself as a thermal insulator. In fact, under given sample preparation conditions, PS can reach a very low thermal conductivity value, owing to the small dimensions of its structures and to the presence of air inside pores. In materials with structures of small dimensions the thermal transport is much reduced with respect to solid macroscopic materials. Moreover, air, which has a very low thermal conductivity, prevents heat transfer between structures.

From these considerations it is evident the interest in measuring the thermal conductivity of PS, under different preparation conditions. The most significant values of thermal conductivity quoted in literature are in ref. [7]. For nanoporous samples (structure size of the order of 3 nm), with porosity of 40%, values as low as 1.2 W/m K are reported, two orders of magnitude lower than that of crystalline silicon, and even lower than the thermal conductivity of silicon oxide (1.4 W/m K).

However the measurement technique described in ref. [7] is rather complicated and cannot be extensively used on different sample types in the experimental steps for the optimization of preparation processes. A heating element and two thermometers are realized directly on the two sides of the sample by thin film technology. Moreover, since the two temperature sensors are directly attached to sample surfaces, these must be covered by an insulating silicon carbide layer. In these conditions, the system under test is a structure SiC/porous Si/Si/SiC, and the effect of SiC layers should be removed from the experimental data.

This paper aims to show that it is possible to use a photoacoustic (PA) technique for the measurement of the thermal conductivity of PS layers with a sufficient accuracy, a relative simplicity and without particular sample treatments. The results refer to PS layers produced by electrochemical etching of crystalline silicon wafers of different type and thickness, in order to get information on the thermal behavior of this material.

1 Experiments

Various photoacoustic methods, in particular gas-microphones techniques, have been successfully applied to study thermal transport in different types of materials, homogeneous and layered. Early applications were made by Adams and Kirkbright, who measured the PA phase as a function of the square root of the angular chopping frequency ω [8]. The procedure adopted in ref. [9] was to measure the attenuation of the amplitude of the thermal oscillation as a function of the root of ω, for rear-surface illumination of the sample. By comparing front-surface and rear-surface illumination, Swimm [10] showed that it is possible to determine the thermal diffusivity of opaque thin films on a transparent substrate. Yasa and Amer [11] and subsequently Pessoa et al. [12] and Thomas et al. [13] showed the validity of a single-frequency method, based on the determination of the attenuation of the rear-surface illumination signal amplitude, with respect to front-surface illumination, or of the relative phase lag between the two illumination types.

In the application here described, the frequency variation of amplitude and phase of the photoacoustic signal are studied, for front-surface illumination of the sample. The evidence of the effect of the PS layer is shown by comparing the values obtained for a p-Si/Si sample to those measured on homogeneous crystalline Si.

The measurement of PS thermal conductivity were performed in a photoacoustic cell of small dimensions (530 mm^3), which consists of a cylindrical aluminum body, delimited by two optical glass windows [14]. The samples are glued to one window in some points by a small amount of adhesive paste, so to leave a thin air space between the window and the substrate. The front surface of the sample is illuminated with the light beam at 514 nm of a Ar^+ ion laser, modulated by an acousto-optic modulator in the frequency range 10 Hz–1 kHz. The experimental results are normalized to the transfer function of the measurement system (cell volume, microphone, preamplifier), which is determined on a carbon black sample [15].

An immediate physical meaning comes out from the behavior of signal amplitude: when increasing modulation frequency, and therefore decreasing the thermal diffusion length in the material, the surface layer of PS gets more and more important in the thermal transport, and the sample surface temperature progressively increases, in reason of the lower thermal conductivity of the layer with respect to that of c-Si substrate.

The absorption is assumed to be localized to sample surface (typically the light absorption coefficient of the investigated samples is in the range 10^3–10^4 cm^{-1}).

As a first approximation, possible effects on PA signal connected to the porosity of material are neglected in this work: in particular the expansion/contraction of the interstitial gas and the effect of light scattering on the heat source distribution in the sample. This is justified since, in the considered frequency range, pore size is orders of magnitude lower than the thermal diffusion length, and the optical absorption coefficient is sufficiently high to neglect scattering phenomena. Therefore, the PS layer is here assumed to behave as a homogeneous material, characterized by its own equivalent thermal conductivity.

Effects of thermoelastic bending, due to a temperature gradient inside the sample, are also neglected. Measurements were made, specifically to verify this assumption, on one of the samples fastened on a window with a blind hole in its center, filled with water, according to a procedure already described in [14]. The results have confirmed the assumed hypothesis; the reason can be attributed to the type of illumination (front) and to the rather low mean sample diffusivity.

The pressure variation in the cell is calculated assuming that the experimental situation can be represented by a four homogeneous layers sample (air, p-Si, c-Si, air) [16]:

$$P(t) = \frac{Q(t)\cdot\mu_g}{k_g\sigma_g + k_p\sigma_p}\cdot\frac{A - B\exp(-2l_p\sigma_p)}{A + B\cdot C\exp(-2l_p\sigma_p)} \tag{1}$$

with

$$A = 1 + \frac{k_g\sigma_g - k_c\sigma_c}{k_g\sigma_g + k_c\sigma_c}\cdot\frac{k_c\sigma_c - k_p\sigma_p}{k_c\sigma_c + k_p\sigma_p}\cdot\exp(-2l_c\sigma_c) \tag{2a}$$

$$B = \frac{k_c\sigma_c - k_p\sigma_p}{k_c\sigma_c + k_g\sigma_p} + \frac{k_g\sigma_g - k_c\sigma_c}{k_g\sigma_g + k_c\sigma_c}\cdot\exp(-2l_c\sigma_c) \tag{2b}$$

$$C = \frac{k_p\sigma_p - k_g\sigma_g}{k_p\sigma_p + k_g\sigma_g} \tag{2c}$$

$Q(t)$ is the heat flux; $\sigma_1 = (1+j)/\mu_i$ where $\mu_i = (2k_i/(\rho_i c_i \omega))^{0.5}$; i = g,c,p respectively for air, c-Si and PS: k_i, ρ_i, c_i, l_i are the thermal conductivity, density, specific heat and thickness of the layers.

2 Results

PS samples with *p* and *n* substrate have been investigated, with different preparation conditions. The first two samples, A and B, were prepared by anodization of *p*-type $\langle 111\rangle$, 0.01 Ω cm wafers, 270 μm thick, in solution ranging from 12 to 20% HF, ethanol and water, with etching parameters showed in Table 1. The two samples have a dark gray color with no evident luminescence and good surface finishing after the air drying process.

Samples C and D were formed by electrochemical anodic etching of *n*-type $\langle 100\rangle$, 10 Ω cm wafers, 500 μm thick, in a solution of 12% HF, ethanol and water, at a current density of 86 mA/cm^2 (see Table 1). The etching was carried on for 720 s for sample C and 3000 s for sample D, in absence of light, in the local breakdown regime at the pore tips. No naked-eye visible luminescence has been observed in the *n*-type samples.

The porous layers thickness were evaluated by SEM measurements. The porosity was estimated by reflectivity measurements [17].

The validity of the model has been tested by comparing the experimental data obtained on single crystal silicon to those obtained by assuming the following parameters: thermal conductivity 156 W/m K; density 2.32 g/cm^3; specific heat 0.713 J/g K. For PS layer the density value is estimated in relation to the porosity; the specific heat value is assumed to be the same as given for

Table 1. PS samples from *p*-type and *n*-type silicon

Sample	A	B	C	D
resistivity (Ω cm)	0.01	0.01	10	10
HF concentration (%)	20	12	12	12
current density (mA/cm^2)	15	15	86	86
time (s)	1800	1800	720	3000
porosity (%)	60	50	40	40
p-Si thickness (μm)	23	10	75	175

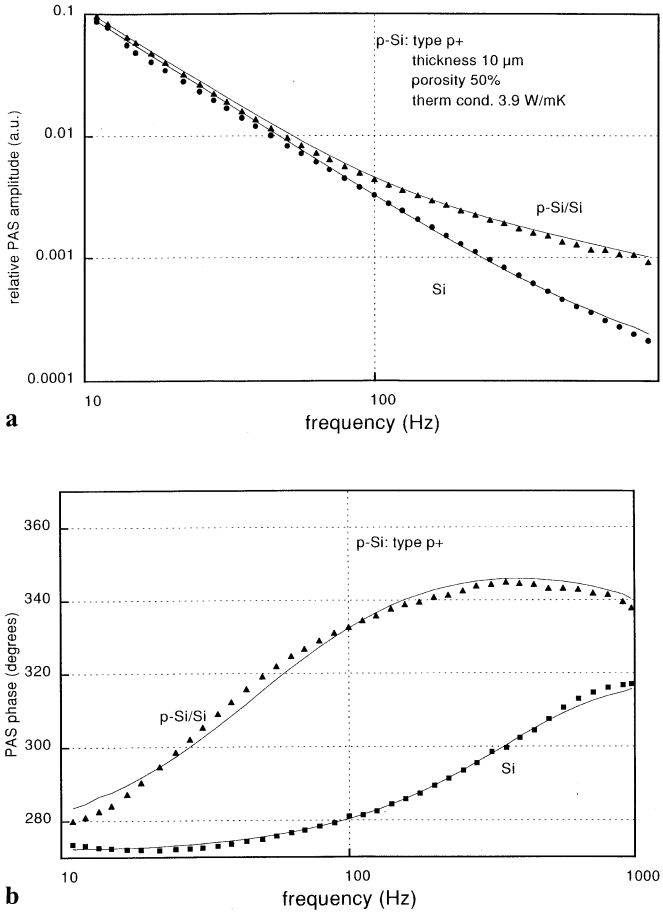

Fig. 1. a Amplitude of PAS signal versus modulation frequency for the crystalline part (●) and the porous part (▲) of sample A; **b** Phase of PAS signal versus modulation frequency for the crystalline part (■) and the porous part (▲) of sample A

c-Si. These approximations give an estimated error on thermal conductivity on the order of 15%.

Figure 1 reports, as an example, the frequency variation of the photoacoustic signal (Fig. 1a, amplitude; Fig. 1b, phase) detected on the porous and crystalline part of sample A, at the same side of the sample. The experimental data are compared with theoretical best-fit curves, on the basis of eq. (1). The thermal conductivity value determined from the fit procedure for PS results 2.5 W/m K. This value is almost two orders of magnitude lower than that of c-Si: this can be attributed to the high porosity of PS layer and to the small dimensions of the structures, on the order of tens of nanometers.

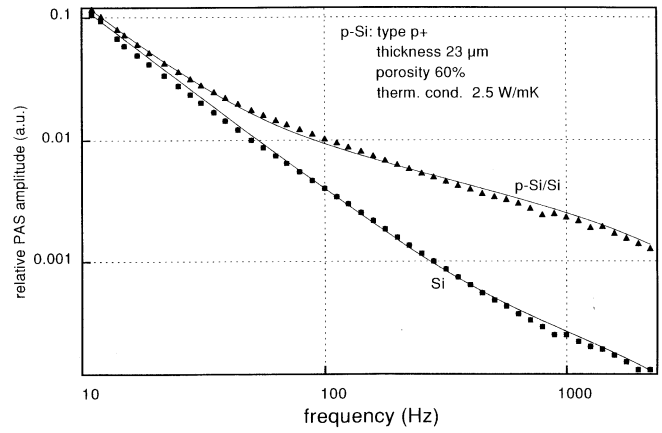

Fig. 2. Amplitude of PAS signal versus modulation frequency for the crystalline part (●) and the porous part (▲) of sample B

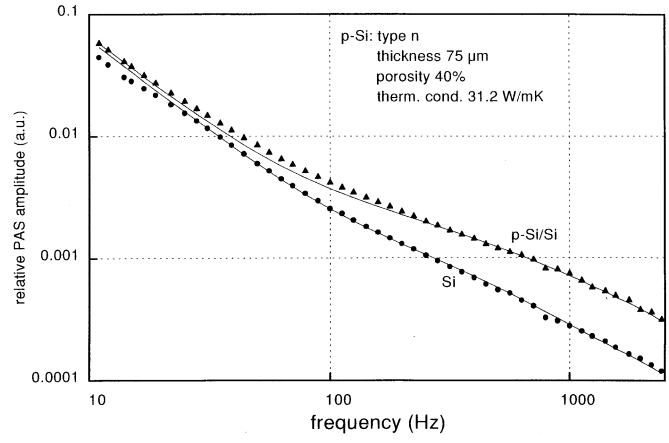

Fig. 3. Amplitude of PAS signal versus modulation frequency for the crystalline part (●) and the porous part (▲) of sample C

Figure 2 refers to sample B. The thermal conductivity value is 3.9 W/m K, higher than that of sample A. In fact both samples A and B are produced from the same substrate type, with the same etching time and current density values, sample B having a little lower porosity due to a lower HF concentration.

Figure 3 refers to sample C, for which the thermal conductivity value obtained from the fit is 31.2 W/m K, about one order of magnitude higher. Sample C is produced from a *n*-type substrate, and therefore the dimension of its structures are about hundred nanometers.

In Fig. 4 the results obtained for sample D are reported, which has been prepared in the same conditions of sample C, but with a different etching time, in order to obtain a larger thickness. In this case, the photoacoustic results are more difficult to interpret. In fact, sample D, owing to its long etching time, has a more heterogeneous morphology. As it can be observed from Fig. 5a, where the SEM image is reported, the sample exhibits different zones: from the surface (on the right) to bulk c-Si (on the left) it is possible to observe a surface layer of a few micrometers [18], a macroporous layer with pores of diameter approximately 500 nm, nearly 35 μm thick

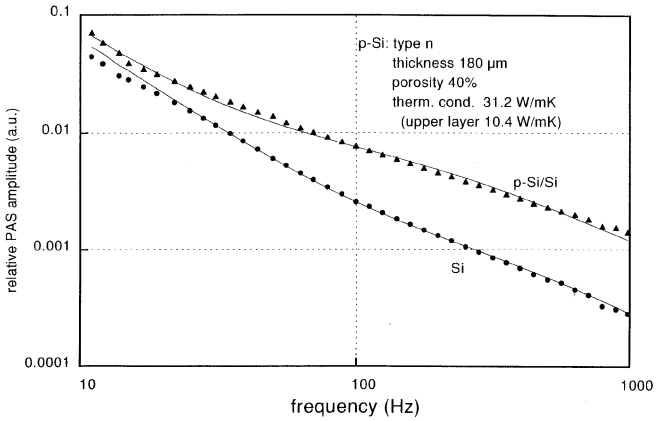

Fig. 4. Amplitude of PAS signal versus modulation frequency for the crystalline part (●) and the porous part (▲) of sample D

(detailed in Fig. 5b), a third porous layer 140 µm thick, with pores of diameter 200 nm (see Fig. 5c), and the crystalline silicon. The third porous layer apparently exhibits different morphologies due to an anomalous section cleavage: in its middle region the cutting plan is not perfectly perpendicular to the surface. For the interpretation of photoacoustic results a tentative has been made by neglecting the thin surface layer, which does not affect the experimental data in the investigated frequency range, and assuming that the other part of the structure can be represented by layers with different thermal conductivity. The best fit procedure has given a thermal conductivity of 10.4 W/m K for the layer with larger pores of dimensions 31.2 W/m K for the layer with lower pores dimensions, equal to that of sample C.

In general, the main limit of the adopted model is the assumption to describe the sample by means of homogeneous layers characterized by discrete variations of thermal conductivity. A more realistic approach should consider the morphology of the porous layer and take into account the distribution of air inclusions within the layer, particularly in the case of thick layers of porous material and at the interfaces air/p-Si and p-Si/c-Si.

3 Conclusions

Since PS is a very promising material in micromachining technology, particulary for the fabrication of thermally

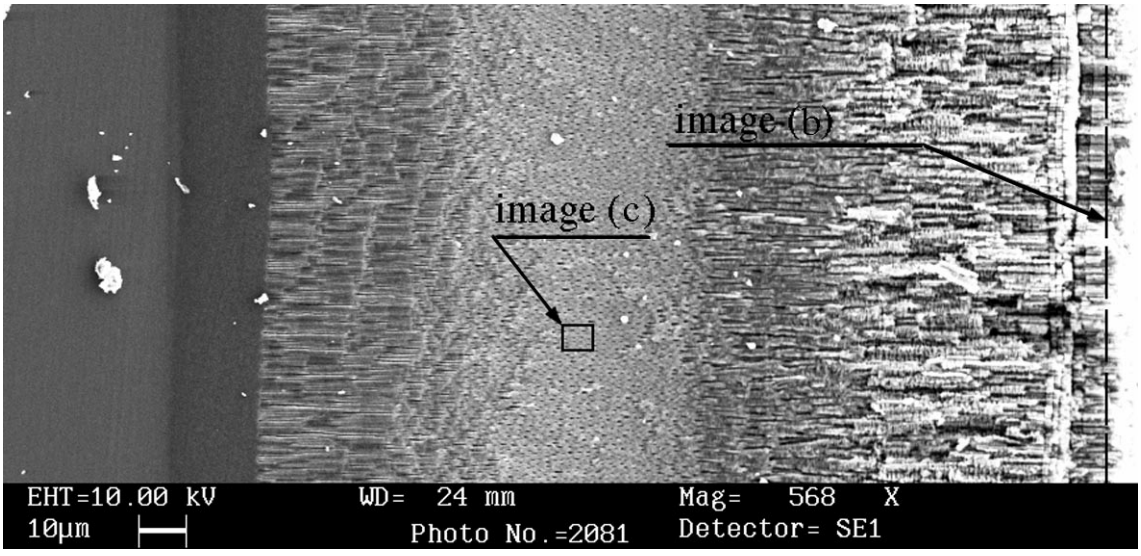

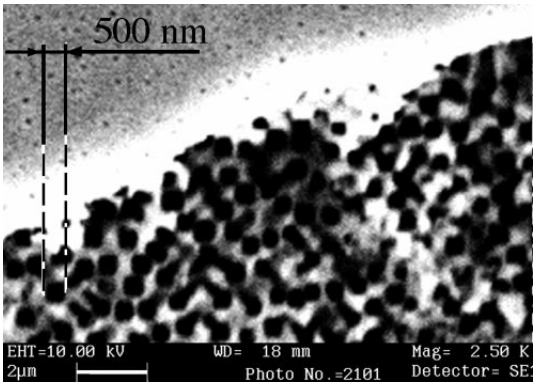

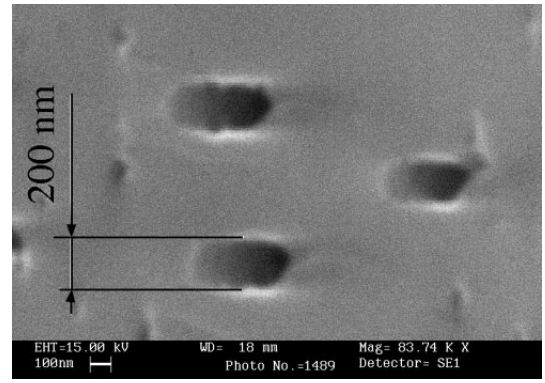

Fig. 5a–c. a SEM cross-section of a 175 µm thick porous layer (sample D) on c-Si. The zones corresponding to the dashed line and the box are detailed in Figs. 5b and 5c; **b** SEM top view of sample D in a purposely delaminated zone: the upper gray part of the image corresponds to the microporous surface layer, the lower part to the macroporous layer; **c** Detailed SEM cross-section of the inset c of a. The oval shape of the pores confirms the oblique cutting angle

insulated structures, it is evident the interest in measuring its thermal conductivity. From this point of view it is very important to implement measurement techniques which can be easily used on different sample types in the experimental steps for the optimization of preparation processes.

In this paper it has been showed that it is possible to determine the thermal conductivity of PS layers by a conventional gas-microphone technique, on the basis of a simple model. It has been showed that, under some preparation conditions, PS can reach very low thermal conductivity values, thus making this material a candidate for the realization of highly insulating layers. An effort should be made to improve the model, in order to consider more realistically the complex morphology of porous layers.

References

1. A. Uhlir: Bell Syst. Techn. J **35**, 333 (1956)
2. L.T. Canham: Appl. Phys. Lett. **57**, 1046 (1990)
3. W. Lang, P. Steiner, A. Richter, K. Marusczyk, G. Weimann, H. Sandmaier: Sensors and Actuators A **43**, 239 (1994)
4. R.C. Anderson, R.S. Muller, C.W. Tobias: J. Microelectromechanical Sys. **3**, 10 (1994)
5. J. Werno, R. Kersjes, W. Mokwa, H. Vogt: Sensors and Actuators A **41**–**42**, 578 (1994)
6. Xiang Zhang, C.P. Grigoropoulos: Rev. Sci. Instrum. 66, 1115 (1995).
7. A. Drost, P. Steiner, H. Moser, W. Lang: Sensors and Materials **7**(2), 111 (1995)
8. M.J. Adams, G.F. Kirkbright: Analyst **102**, 281 (1977).
9. P. Charpentier, F. Lepoutre, L. Bertrand: J. Appl. Phys. **53**, 608 (1982)
10. R.T. Swimm: Appl. Phys. Lett. **42**, 955 (1983)
11. Z. Yasa, N. Amer: Topical Meeting on Photoacoustic Spectroscopy, Paper WA 5–1, Ames, Iowa (1979)
12. O. Pessoa, C.L. Cesar, N.A. Patel, H. Vargas, C.C. Guizoni, L.C.M. Miranda: J. Appl. Phys. **59**, 1316 (1986)
13. S. Thomas, J. Isaac, J. Philip: Rev. Sci. Instrum. **66**, 3907 (1995).
14. G. Amato, G. Benedetto, R. Spagnolo, M. Turnaturi: Phys. Stat. Sol. (a) **114**, 519 (1989)
15. G. Benedetto, R. Spagnolo: Appl. Phys. A **46**, 169 (1988)
16. J. Baumann, R. Tilgner: Can. J. Phys. **64**, 1291 (1986)
17. C. Pickering, M.I.J. Beale, D.J. Robbins, P.J. Pearson, R. Greef: J. Phys. C **17**, 6535 (1984)
18. V. Lehmann, H. Föll: J. Electrochem. Soc. **137**, 653 (1990).